Proceedings of the 33rd
Conference on Decision and Control
Lake Buena Vista, FL - December 1994

Robust Control of a Catalytic Fixed Bed Reactor

A. Kremling and F. Allgöwer *
Institut für Systemdynamik und Regelungstechnik
Universität Stuttgart
70550 Stuttgart, Germany

Abstract

Catalytic fixed bed reactors exhibit interesting control problems due to their nonlinear behaviour and their sensitivity to load changes and other disturbances. Because detailed nonlinear models of such reactors are too complex for use in controller design, a linear model description is identified here along with an appropriate structured uncertainty description. The controller is designed based on the μ-paradigm to guarantee robust stability and robust performance. A comparison with an H_∞-optimal controller is also given. For the H_∞-design the structured uncertainties are converted into a single multivariable unstructured uncertainty. As expected the H_∞-controller can only achieve a much less demanding performance because of the conservatism of the unstructured uncertainty description. Experimental results involving a real reactor are given.

1. Introduction and Process Description

Catalytic fixed bed reactors are the most widely used reactor type for gas phase reactants and play an important role in chemical industries. Interesting control problems arise due to their nonlinear and distributed behaviour [6].

In this paper we consider control of a fixed bed reactor for Formaldehyde synthesis in laboratory scale. The plant oxidizes Methanol CH_3OH and Oxygen O_2 to the desired product Formaldehyde $HCHO$ which is an important primary product in the plastic industry. In a consecutive reaction Formaldehyde is further converted to the unwanted byproduct carbon monoxide CO. The experimental plant consists of the feed preparation of the gases included the mixer and the Methanol valve, the reactor with a cooling jacket which is divided in three sections each connected with a thermostat, the absorption column and a process control system for process monitoring, operation and control.

The main reactions take place at the catalyst surface in the reactor. The reaction rate depends on several factors including the temperature. Both reactions are exothermic, i.e. heat is being produced. Thus a characteristic temperature profile forms along the longitudinal axis of the reactor. The reactor can therefore be considered as a system with distributed parameters. The process is operated such that an isothermic temperature profile is formed in the reactor, i.e. the steady-state temperature does not vary along the reactor axis. This results in an even load on the whole catalyzer and guarantees good conversion.

Control problem: The process is very sensitive to load changes or other disturbances. Therefore control of the temperature profile is necessary to obtain a constant space time yield of Formaldehyde. The influence of the inlet temperature T_{in} and the gas throughput Q are considered as disturbances. The setpoint of the first thermostat Th_1 and the Methanol-Oxygen ratio MR are selected as control inputs. These two inputs have the strongest effect on the temperature profile. Two temperature measurements T_{m1} and T_{m2} are chosen as measured outputs. The position of the temperature measurements is at locations that allow to infer the form of the profile in a wide range. Thus control of the temperatures T_{m1} and T_{m2} will result indirectly in good control of the whole profile. Through this inferential control scheme we have thus reduced the problem of controlling a distributed output to the control of two lumped outputs.

In order to make controller synthesis possible, we identify a lumped parametric linear system that describes the dynamics in a small neighbourhood around the main operating point rather well. This is not true any more if disturbances are present and the reactor state leaves the immediate neighbourhood of the main operating point. Therefore a robust controller is needed in order to maintain stability and performance during actual operation. Because different parts of the plant, like the feed preprocessing, the thermostats and the reactor, can be identified independently and because the uncertainties of each of these parts varies significantly in size, we describe the uncertainties in a structured way: For each part of the plant, a separate linear nominal model and linear uncertainty description is identified. This structured uncertainty can be used in a μ-optimal controller design in order to achieve a satisfactory robust-

*author to whom all correspondence should be addressed: phone +49-711-6856193, fax +49-711-6856371, email: allgower@rus.uni-stuttgart.de

ness. Of course no robustness *guarantee* can be given for the real reactor, as the real plant is a nonlinear distributed system and only linear uncertainties are taken into account. With results at the real plant we show however that robustness of stability and performance is indeed achieved by this approach.

2. Linear Model Identification

The linear process model to be identified consists of a transfer matrix G_s, which describes the influence of the control inputs $\mathbf{u}$ (setpoint of Th_1, Methanol-Oxygen ratio MR) on the controlled outputs $\mathbf{y}$ (T_{m1},T_{m2}), and a transfer matrix G_z, describing the effect of disturbances in the feed $\mathbf{z}$ (inlet Temperture T_{in}, gas throughput Q) on the outputs $\mathbf{y}$

$$\mathbf{y} = G_s\mathbf{u} + G_z\mathbf{z} \tag{1}$$

Both G_s and G_z are (2,2)-matrices. The disturbance model G_z is used for μ-optimal controller design. During the identification phase we have access to two further measurements, namely the temperature T_{c1} of the coolant at the exit of the first cooling jacket and the amount of Methanol flowing into the mixer. This will allow us to identify the dynamics of the thermostat Th_1 and the dynamics of the Methanol valve separately from the dynamic of the actual reactor. Transfer matrix G_s is therefore divided into two systems connected in series:

$$G_s(s) = H'(s) \cdot P'(s) \tag{2}$$

System P' describes the dynamics of the two "actuators" (thermostat Th_1 and Methanol valve) that are independent of each other. System H' is the dynamic model of the actual reactor.

It turns out that the dynamics of the Methanol valve can be described with sufficient accuracy by a constant gain k_{mv}. Transfer matrix P' is thus a diagonal matrix with only one dynamic element $p_{11}(s)$:

$$P'(s) = \begin{pmatrix} p_{11}(s) & 0 \\ 0 & k_{mv} \end{pmatrix} \tag{3}$$

For simplicity the constant k_{mv} is included in the reactor dynamics leading to

$$G_s(s) = H(s) \cdot P(s) \tag{4}$$

with

$$P(s) = \begin{pmatrix} p_{11}(s) & 0 \\ 0 & 1 \end{pmatrix} \tag{5}$$

and

$$H(s) = H'(s) \cdot \begin{pmatrix} 1 & 0 \\ 0 & k_{mv} \end{pmatrix} = \begin{pmatrix} h_{11}(s) & h_{12}(s) \\ h_{21}(s) & h_{22}(s) \end{pmatrix} \tag{6}$$

Each dynamic element in (5) and (6) is identified separately. We will show below that for each element an additive uncertainty description [8], covering the uncertainties present, can be found. The real plant is thus assumed to consist of nominal model (4) plus additive dynamic uncertainties

$$G_{sreal} = \begin{pmatrix} h_{11} + \Delta_{11}\, h_{a11} & h_{12} + \Delta_{12}\, h_{a12} \\ h_{21} + \Delta_{21}\, h_{a21} & h_{22} + \Delta_{22}\, h_{a22} \end{pmatrix} \begin{pmatrix} p_{11} + \Delta_{p1}\, p_{a1} & 0 \\ 0 & 1 \end{pmatrix} \tag{7}$$

Perturbations Δ_{ij} can be arbitrary, stable, dynamic SISO-systems satisfying

$$||\Delta_{ij}||_\infty \leq 1 \tag{8}$$

The frequency dependent size of the different uncertainty terms is captured in quantities h_{aij} and p_{a1} that are determined below.

Pseudo Random Binary Signals (PRBS) are used to collect the input-output data used for identification.

Data are collected from different experiments at different operating points with different PRBS amplitudes. These operating points are characterized by the same temperature profile as at the main operating point, but with different composition and temperature of the feed, and different stationary value of the control input $\mathbf{u}$. Persistent, i.e. non-vanishing, disturbances in the controlled closed loop will lead to such operating points.

The nominal model is identified from averaged data in order to give a good "average" description of the dynamic behavior. Identification is performed with the System Identification Toolbox [7] in MATLAB. Figure 1 shows a typical excitation signal, resulting measured outputs T_{mi} and responses of the identified transfer functions for the elements of p_1, h_{11} and h_{21} of (5) and (6). The resulting discrete time systems are converted into continuous time using a Tustin transformation. The so identified nominal model is of total order 16 and has 4 zeros with positive real parts. Nominal model G_s shows strong dynamic interactions. By a suitable scaling of the inputs and outputs the condition number can be reduced to a value of 2.8. Identification of the nominal disturbance transfer functions is done in a similar way.

To obtain uncertainty description (7), different models, resulting from identifications with input-output data acquired with different PRBS inputs at different operating points, are drawn into one Bode plot for each SISO transfer function $g(s)$. Figure 2 shows exemplary the nominal model (solid line), and some models identified at different operating points (dotted lines) for transfer function h_{11}. The dashed lines in Figure 2 give an upper and lower bound on

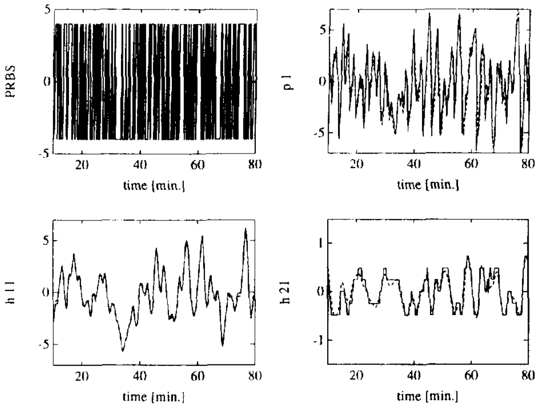

Figure 1: Exitation signal, measured outputs T_{mi} (–) and response of the identified transfer functions (– –) for elements p_1, h_{11}, h_{21}.

the frequency dependent gain and phase of all models obtained for this element.

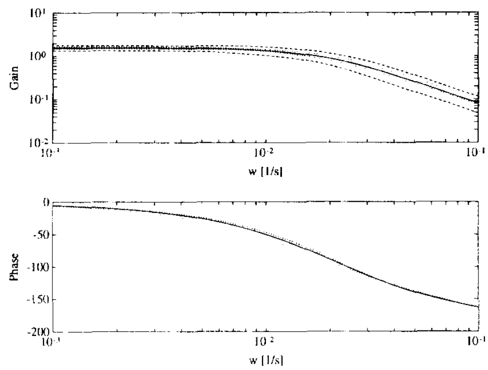

Figure 2: Amplitude and phase plots at different operating points for element h_{11}.

With these bounds the gain and phase for each frequency ω_i can be described by a nominal term $A_{nom}(\omega_i)$ and $\phi_{nom}(\omega_i)$ and an uncertain term that can be bounded in size:

$$A(\omega_i) = A_{nom}(\omega_i) + \Delta_A(\omega_i) \tag{9}$$

$$\phi(\omega_i) = \phi_{nom}(\omega_i) + \Delta_\phi(\omega_i) \tag{10}$$

with

$$|\Delta_A(\omega_i)| \leq A_\Delta(\omega_i) \tag{11}$$

$$|\Delta_\phi(\omega_i)| \leq \phi_\Delta(\omega_i) \tag{12}$$

Gain and phase uncertainty (9) and (10) is converted next to a (complex) additive uncertainty for transfer function $g(j\omega)$

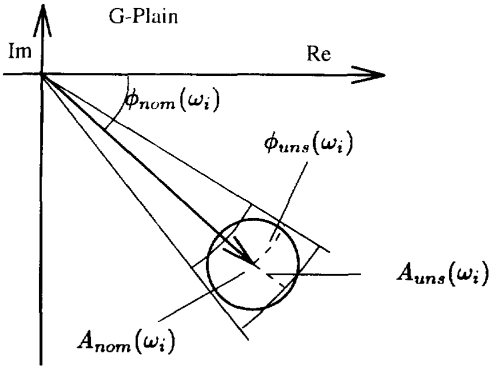

Figure 3: Approximation of the gain/phase-uncertainty by a norm bounded complex uncertainty.

$$g(j\omega) = g_{nom}(j\omega) + \Delta(j\omega) \cdot L_A(j\omega) \tag{13}$$

where Δ is an arbitrary dynamic system with gain smaller or equal to one

$$|\Delta(j\omega)| \leq 1 \qquad \forall\, \omega \tag{14}$$

and $L_A(j\omega)$ is an uncertainty weight to be determined. The information on the size of the uncertainty is contained in $L_A(j\omega)$.

Gain and phase uncertainty for one frequency point is given by the circular segment in Figure 3. The real value for $g(j\omega_i)$ is located somewhere in this segment. This segment can be approximated by a suitable circle as shown in Figure 3. The radius of this circle gives the modulus of the wanted weight $\bar{L}_A(\omega_i)$ for this frequency. $\bar{L}_A(\omega_i)$ taken for different frequencies ω_i gives the frequency dependent weight $\bar{L}_A(\omega)$. A stable minimum phase transfer function $L_A(j\omega)$, having $\bar{L}_A(\omega)$ as its gain, can be easily found, rendering the sought after uncertainty weight $L_A(j\omega)$ in (13). Figure 4 shows exemplary radius $\bar{L}_A(\omega)$ derived for h_{11}. This derivation of the additive uncertainty is performed for all uncertain transfer functions in (7).

There are various sources of conservatism in this approach to determine the uncertainty description: Starting out with bounds on the gain and phase in the Bode plots is of course conservative. The step from these bounds to description (9) and (10) is potentially conservative if the upper and lower bounds in the Bode plot are not equally "distributed" around the respective nominal values. Finally approximating the circular segment by a circle can be rather conservative if the gain and phase uncertainty are very different in size. We want to stress however, that this

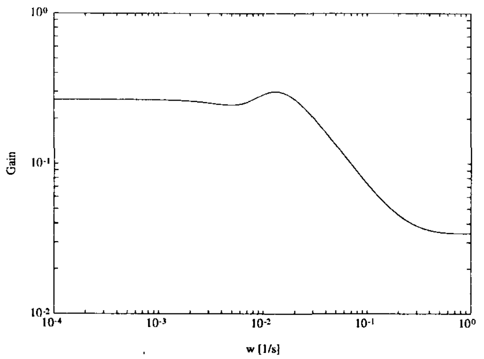

Figure 4: Uncertainty radius $\bar{L}_A(\omega)$ for transfer function h_{11}.

is not a problem here. The biggest effect on reducing conservatism is achieved by splitting the plant transfer matrix in an "actuator part" P with large uncertainty and the actual reactor H with moderate uncertainty.

3. Robust Controller Design for the Fixed Bed Reactor

μ-Optimal Control of the Reactor

In Section 2 the plant model including disturbance model and structured uncertainty description is derived. In this section we synthesize a robustly stabilizing controller using the μ-paradigm that guarantees a certain performance for all plants within the uncertainty description. An excellent introduction into μ-optimal control theory can for example be found in [4] and [8].

Our main objective is to attenuate the effect of disturbances in the feed (inlet temperature T_{in} and gas throughput Q) on the temperatures T_{m1} and T_{m2} and thus maintaining the desired isothermal temperature profile in the reactor. The reactor has the tendency to oscillations with frequencies in the vicinity of the desired bandwidth. These oscillations are very undesirable during operation because they result in an unsteady quality of the desired product. Therefore we penalize control action in the frequency range around $\omega = 10^{-3}[1/s]$. These objectives can be expressed as H_∞-specifications as follows:

$$\left\| \begin{array}{c} W_1 \cdot S \cdot G_z \\ W_2 \cdot KS \cdot G_z \end{array} \right\|_\infty < 1 \qquad (15)$$

Weights W_1 and W_2 are chosen to quantify the desired performance. Weight W_1 is a low-pass filter (Figure 5) with steady state gain chosen to guarantee a steady state offset for the worst disturbance that is smaller than the resolution of the temperature measurement. Furthermore the bandwidth and maximal disturbance amplification are determined with W_1. Weight W_2 is chosen as a bandpass filter penalizing control action in the neighbourhood of the desired bandwidth.

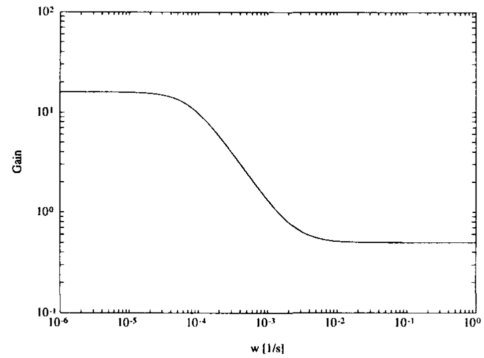

Figure 5: Singular values of performance weight W_1.

This problem can be easily transformed into the M-Δ-structure [8] needed for the μ-analysis and synthesis. Standard D-K-iteration [5, 3], starting with a D-matrix set to the identity matrix, does not converge to a solution. By H_∞-loop-shaping a controller is formed that is used to calculate better suited D-matrices to initiate D-K-iteration. This controller is not aimed at satisfying performance condition (15), but to 'guide' the algorithm into the right direction. Synthesis weights W_{1syn} and W_{2syn} used for controller synthesis are chosen somewhat different to performance weight W_1 and W_2 in (15), in order to stress the achievement of certain specifications over others [1, 2]. Here the desired bandwidth and maximal disturbance amplification are chosen more demanding in order to stress achievement of performance over stability in this respect. D-K-iteration converges to the controller shown in Figure 6 after three further iteration steps.

The resulting controller is of order 73, that can be reduced to order 15 without loss of performance or robustness. Figure 7 shows the graph of μ for robust performance and robust stability for performance specification (15). As can be seen the μ-optimal controller guarantees robust stability with respect to the uncertainties described. Robust performance is not completely met, as $\mu(M) > 1$ for some frequencies in the neighbourhood of the bandwidth. For the practical application at hand this result is however completely satisfactory and no further redesign is needed. This controller is implemented on the DCS at the real plant. Figure 8 shows the closed loop behaviour of the so-controlled laboratory plant to simultaneous disturbances in the inlet temperature by $-20\,K$ and in the throughput by $+1\,\%$.

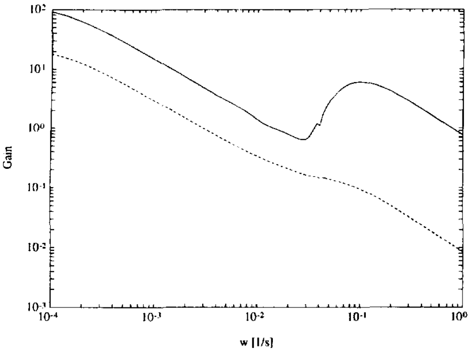

Figure 6: Singular values of μ-optimal controller.

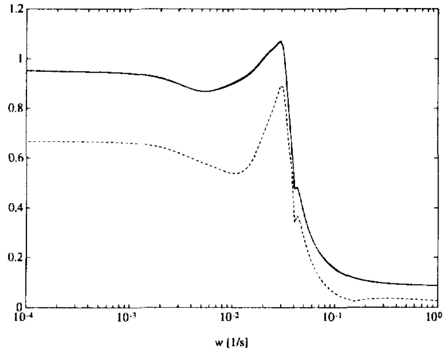

Figure 7: μ for robust performance (solid line) and robust stability (dashed line) for the μ-optimal controller.

From physical arguments and experience, the chosen disturbance is known to have the strongest effect on the temperature profile. It is worth mentioning that the physically motivated worst disturbance is equivalent to the systemtheoretic one that can be found by a singular value decomposition of G_z. This sustains the good quality of the identified model. The performance of the closed loop is much improved compared to specifications achieved with industrial-type PI-controllers. As intended no pronounced oscillations in the reactor are observed. The μ-controller designed shows a very even performance for differently perturbed plants in simulation and at the real plant for different operating conditions.

H_∞-Optimal Control of the Reactor

In order to see the advantages gained by using a structured uncertainty description as compared to an unstructured description, the controller derived in Section 3.1 is compared to an H_∞-controller. First an unstructured uncertainty description (Figure 9) is de-

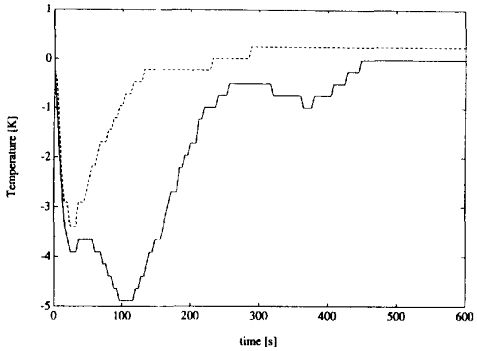

Figure 8: Closed loop behaviour of the real plant with the μ-optimal controller. Temperatures T_{m1} (solid line) and T_{m2} (dashed line).

duced, that contains the structured uncertainties but is not unnecessarily conservative. In a first step the

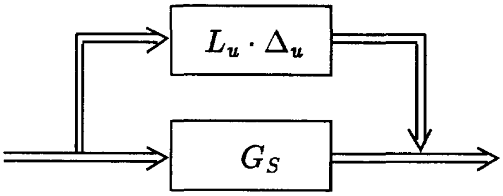

Figure 9: System with unstructured additive uncertainty.

(1,1)- and (2,1)-elements of G_s are found by looking at the series connection of h_{11} and p_1 and h_{21} and p_1 respectively (compare eq. (4)):

$$(h_{11} + \Delta_{s11} \cdot h_{a11}) \cdot (p_1 + \Delta_{s1} \cdot p_{a1}) = \underbrace{h_{11} \cdot p_1}_{g_{11}}$$

$$+ \underbrace{\Delta_{s11} \cdot h_{a11} \cdot p_{s1} + h_{11} \cdot \Delta_1 \cdot p_{a1} + \Delta_{s11} \cdot h_{a11} \cdot \Delta_{s1} \cdot p_{a1}}_{\Delta_{u11} \cdot g_{a11}}$$

$$|\Delta| \leq 1 \quad \forall\, \omega \qquad (16)$$

where the norm bounded uncertainties Δ_s are the structured perturbations and Δ_u is the resulting unstructured perturbation. It is straightforward to calculate an upper bound on $g_{a11}(\omega)$ and fit a stable, minimum phase transfer function $g_{a11}(j\omega)$ for the magnitude data $g_{a11}(\omega)$. This step is performed for g_{11} and g_{21}. Transfer functions g_{12} and g_{22} are equal to l_{12} and l_{22} (4). Now we have a 2x2 transfer matrix G_s with additive uncertainties in all four elements:

$$G_s = \begin{pmatrix} g_{11} + \Delta_{s11}\, g_{a11} & g_{12} + \Delta_{s12}\, g_{a21} \\ g_{21} + \Delta_{s21}\, g_{a21} & g_{22} + \Delta_{s22}\, g_{a22} \end{pmatrix}$$

$$|\Delta_{sij}| \leq 1 \quad \forall\, \omega \quad (17)$$

In the next step we want to find a multivariable additive uncertainty description:

$$G_s = \begin{pmatrix} g_{11} & g_{12} \\ g_{21} & g_{22} \end{pmatrix} + L_u \cdot \Delta_u \; ; \quad \bar{\sigma}(\Delta_u) \leq 1 \quad \forall\, \omega \tag{18}$$

with L_u being a 2x2 multivariable uncertainty weight such that robustness with respect to (18) guarantees robustness with respect to (17). In other words, uncertainty description (18) must 'cover' uncertainty description (17). In order to derive L_u we proceed in two steps: First (17) is brought into a form where each element of G_s depends on the different perturbation terms in Δ_u, e.g.

$$g_{11} + l_{u11}\Delta_{u11} \; + l_{u21}\Delta_{u12} \tag{19}$$

It can be shown in a second step that the following values for l_{uij}

$$\begin{aligned} |l_{u11}| &= \max\{|l_{a11}|, |l_{a21}|\} \\ |l_{u21}| &= \max\{|l_{a11}|, |l_{a21}|\} \\ |l_{u12}| &= \max\{|l_{a12}|, |l_{a22}|\} \\ |l_{u12}| &= \max\{|l_{a12}|, |l_{a22}|\} \end{aligned} \tag{20}$$

guarantee that (19) covers (17). Now a multivariable stable minimum phase system $L_u(s)$ can be fit to the magnitude data of equations (20). Of course (18) is a more conservative uncertainty description than (17). Bounds (20) are however such that no *unnecessary* conservatism is introduced.

In order to guarantee robustness of stability with respect to the uncertainties (18) the following H_∞-norm bound has to be satisfied [8]:

$$\| \; L_u \cdot KS \; \|_\infty < 1 \tag{21}$$

In order to attenuate the effect of disturbances in the feed on the controlled outputs T_{m1} and T_{m2},

$$\| \; W_s \cdot S \; \|_\infty < 1 \tag{22}$$

has to hold, where W_s reflects the desired performance (Figure 10).

Specifications (21) and (22) are met if a controller is found so that

$$\left\| \begin{array}{c} W_s \cdot S \\ L_u \cdot KS \end{array} \right\|_\infty < 1 \tag{23}$$

holds. It should be noted that disturbance model G_z cannot be considered in (22) because weighting of $L_u \cdot KS$ by G_z does not guarantee robustness of stability any more. Also note that $L_u \cdot KS$ in (23) is needed to achieve robust stability, while $W_2 \cdot KS \cdot G_z$ in (15) is included as a performance specification (suppression of unwanted oscillations). Oscillations are nevertheless also not expected for H_∞-controllers satisfying (23) because $L_u \cdot KS$ will have a similar effect on u as $W_2 \cdot KS \cdot G_z$.

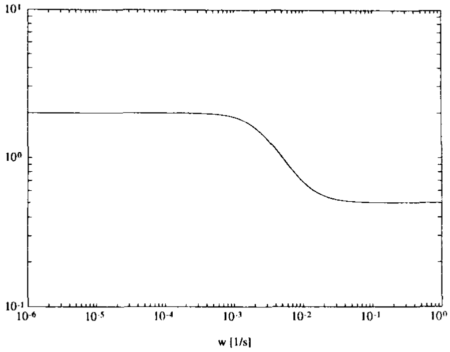

Figure 10: Singular values of performance weight W_S.

Figure 11 shows the singular values of an H_∞-controller satisfying (23) and thus guaranteeing robust stability (22) and nominal performance (21). When comparing Figures 11 and 6 it is clear that the H_∞-controller is much more 'cautious' (low gain for low frequencies) than the μ-optimal controller. This is due to the large uncertainty at low frequencies.

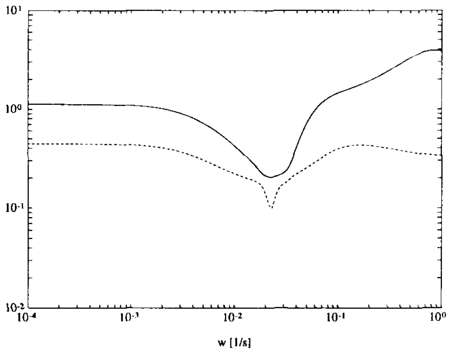

Figure 11: Singular values of the H_∞-suboptimal controller.

For analysis purposes the μ-plot of the H_∞-controller with performance objective (15) (that was used in μ-controller design) and structured uncertainty description is depicted in Figure 12. The H_∞-controller is very conservative in the frequency range around the bandwidth due to the conservatism of the unstructured uncertainty description. Robust stability is obviously overemphasized in this design (small value of $\mu(M_{11})$—dashed curve in Figure 12). For low frequencies robust performance can not be met by far. Thus a large steady state error is expected. Figure 13 compares the closed loop behaviour of the

H_∞-controlled and μ-controlled real plant, when the worst-case disturbance as discussed in Section 3.1 is applied. As expected the H_∞-controller is also stable but does not achieve the same level of performance as the μ-controller does.

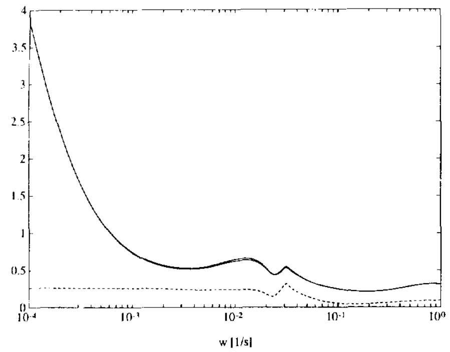

Figure 12: μ for robust performance (solid) and robust stability (dashed) for the H_∞-suboptimal controller.

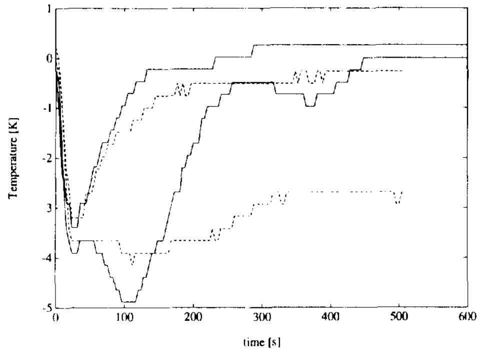

Figure 13: Comparison of the closed loop behaviour (temperatures T_{m1} and T_{m2}) of the H_∞-controlled (dashed line) and μ-controlled (solid line) real plant.

4. Conclusions

This paper describes application of μ-optimal controller design to control of an important chemical process, namely synthesis of Formaldehyde in a catalytic fixed bed reactor. This process is a nonlinear system with distributed parameters. It is however possible to describe this reactor by a linear real-rational nominal transfer matrix and a (linear) uncertainty description. One important source of uncertainty, the dynamics of thermostat Th_1, can be captured separately. Also each element of the multivariable transfer function is identified separately, leading to an independent uncertainty description for each element. A practical method for obtaining the uncertainty description was shown.

A μ-optimal controller was designed on the basis of this structured uncertainty description to robustly attenuate the effects of disturbances on the controlled outputs and to suppress unwanted oscillations in the reactor. With results from the real plant it was shown, that the desired performance is indeed achieved with this controller.

In order to see the benefits gained by the structured consideration of uncertainties, the μ-optimal controller is compared to an H_∞-controller, that is based on an unstructured uncertainty description. A method was shown how to derive the unstructured uncertainty description from the structured one. Comparison between the μ-controlled and H_∞-controlled real plant shows clearly the advantage gained from the structured uncertainty description.

This case study shows, that the increased effort needed for derivation of the structured uncertainty description and μ-optimal controller design might well pay off due to an improved performance achieved and due to the robustness assurance that can be given when compared to H_∞-optimal controllers and traditional controller designs used in chemical industries.

References

[1] N. Amann and F. Allgöwer. Design of robustly performing controllers for a class of practical control problems. In 2nd European Control Conference, *Groningen, NL*, pages 721–726, 1993.

[2] N. Amann and F. Allgöwer. μ-suboptimal design of a robustly performing controller for a chemical reactor. *Int. J. Control*, volume 59 (3), pages 665–687, 1994.

[3] G.J. Balas, J.C. Doyle, K. Glover, A. Packard, and R. Smith. *μ-Analysis and Synthesis Toolbox (μ-Tools).* MUSYN Inc., Minneapolis, 1991.

[4] J.C. Doyle. Analysis of feedback systems with structured uncertainties. *IEE Proceedings, Part D*, 129(6):242–250, 1982.

[5] J.C. Doyle and C.-C. Chu. Matrix Interpolation and H_∞-Performance Bounds. In *Proc. 1985 American Control Conference*, pages 129–134, Boston, MA, 1985.

[6] S. B. Jørgensen, Fixed Bed Reactor Dynamics and Control – A Review. In *Dycord 86*, IFAC, pages 11 – 24, 1986.

[7] L. Ljung. *System Identification Toolbox for use with MATLAB.* The MathWorks, Inc., South Natick, MA, 1992.

[8] M. Morari and E. Zafiriou. *Robust Process Control.* Prentice-Hall, 1989.